

Fabrication and Characterization of Silver/Polyaniline Composite Nanowires in Porous Anodic Alumina

Anna Drury,^{*,†} Shweta Chaure,^{†,§} Michael Kröll,^{†,#} Valeria Nicolosi,[†] Nandu Chaure,[‡] and Werner J. Blau[†]

School of Physics, University of Dublin, Trinity College, Dublin 2, Ireland, and University of Sheffield, Sheffield, UK, Faculty of ACES, Sheffield Hallam University, Pond Street, Sheffield S11WB, United Kingdom

Received April 24, 2007. Revised Manuscript Received May 30, 2007

Silver/polyaniline (Ag/PANI) nanowires are prepared by electropolymerization of aniline in porous anodic aluminum oxide (AAO) from an acidic electrolyte containing silver metal ions and aniline. Ag nanowires, PANI nanowires, and PANI thin films are made for comparative purposes. The nanowires are characterized by scanning electron microscopy (SEM), transmission electron microscopy (TEM), high-resolution transmission electron microscopy (HRTEM) and X-ray diffraction. The HRTEM images illustrate that the composite nanowires consist of core Ag nanowires sheathed by polymer; i.e., they are nanocables. UV–visible absorption spectroscopy (UV–vis), Fourier transform infrared spectroscopy (FTIR), and Raman spectroscopy are done to investigate the chemical structure of the nanocables and any interaction between Ag and PANI. The Raman spectra indicate that the polymer is in the conducting emeraldine salt form and FTIR shows that there is some interaction between Ag and the acid protonated NH groups of polyaniline.

1. Introduction

There is currently considerable interest in fabricating nanostructured organic–inorganic hybrid materials. Doping with a suitable material can alter the properties of many molecules such as polymers. Metal/polymer composites are particularly useful, as they combine the electrical characteristics of metals and the mechanical and processing properties of polymers.¹ Many of these composites show enhanced electrocatalytic activity and increased gas sensing properties.^{2,3} A polymer coating on a metal nanowire would have the further advantage of protecting the nanowire from oxidation and corrosion.

Conducting polymers have also been extensively studied during the past decade. Polyaniline (PANI) is often chosen because of its stability in air and its electrical, electrochemical, and optical properties⁴ and many useful devices such as chemical and biological sensors, batteries, infrared polarizers, and light emitting diodes have been made from it. PANI can be synthesized in several insulating forms shown in Figure 1.

Conducting polyaniline is achieved by doping the EB with a protonic acid to give the structure in Figure 2.

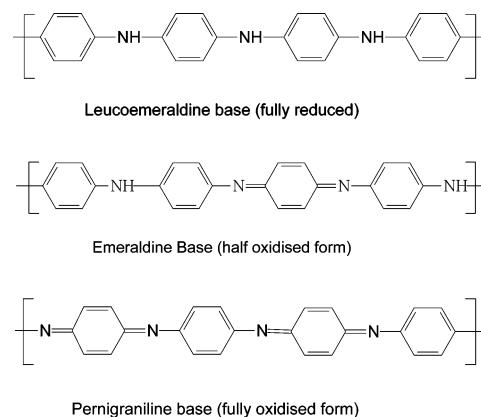


Figure 1. Base forms of PANI; leucoemeraldine base (LEB), emeraldine base (EB), and pernigraniline base (PNB).

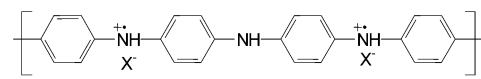


Figure 2. Oxidized bi-polaronic emeraldine salt (ES).

It is also possible to synthesize polyaniline nanotubes from aniline by self-assembly using a protonic acid as an external dopant.⁵ Nanostructures of conducting polymers synthesized by the template methods have been shown to have electrical conductivities well above those of powder or thin film forms of the same polymer⁶ and have many potential applications in nanodevices.⁷ As well as potential applications of nanomaterials for device structures, they are also of fundamental

* To whom correspondence should be addressed. E-mail: adrury@tcd.ie. Fax: 0035316711759.

[†] University of Dublin.

[‡] University of Sheffield.

[§] Present address: Department of Materials, Queen Mary, University of London, Mile End Road, London E1 4NS, UK.

[#] Present address: Degussa GmbH, Aerosil and Silanes, 63457 Hanau, Germany.

(1) Bhattacharya, S. K., Ed. *Metal-filled polymers (properties and applications)*; Dekker: New York, 1986.

(2) Malinauskas, A. *Synth. Met.* **1999**, *107*, 75–83.

(3) Musiani, M. *Electrochim. Acta* **2000**, *45*, 3397–3402.

(4) MacDiarmid, A. G.; Kaner, R. B. In *Handbook of Conducting Polymers*; Skotheim, T. A., Ed.; Marcel Dekker: New York, 1986; Vol. 1, p 718.

(5) Wei, Z. X.; Zhang, L. J.; Yu, M.; Yang, Y. S.; Wan, M. X. *Adv. Mater.* **2003**, *15*, 1382–1385.

(6) Wang, C.; Wang, Z.; Li, M.; Li, H. *Chem. Phys. Lett.* **2001**, *341*, 431–434.

(7) Heeger, A. J. *J. Phys. Chem. B* **2001**, *105*, 8475–8491.

interest. Nanowires of conjugated polymers are ideal systems for studying 1D confinement effects on optical, electronic, and electron transport properties.

It has been shown that the incorporation of metal and metal oxide particles into conducting polymer films enhances their electrocatalytic activity and other properties.⁸ Various techniques have been used to incorporate metallic nanoparticles (such as gold, copper, platinum, and palladium) into polymer matrixes.⁹ It is possible to introduce metals into the PANI polymer system via the lone pair of electrons on the nitrogen. Many PANI/metal nanoparticles have been shown to possess enhanced sensing and catalytic capabilities compared to pure PANI (ref 10 and references therein).

Silver (Ag) exhibits the highest electrical and thermal conductivity among all metals. It is also known for its antibacterial properties and its ability to promote surface-enhanced optical phenomena.¹¹ Silver nanoparticles in particular show enhanced catalytic activity, high electrical conductivity, and unique optical properties⁸ and are used in a variety of applications such as optical and electrical nanodevices and nanosensors.¹² Many chemical and physical methods have already been used to incorporate silver nanoparticles into polymer films;¹³ however, homogeneous dispersion into the polymer matrix is difficult as suspensions or dispersions of silver nanoparticles tend to aggregate.¹⁴ Recently, self-doping polyaniline nanotubes with silver nanoparticles assembled along them have been made.¹⁵ Khanna et al. have also prepared Ag/PANI nanocomposites by a photochemical reaction.¹⁶

We have developed a method of preparing Ag/PANI composite nanowires into the pores of an anodic alumina membrane (AAO) by simultaneous oxidative electropolymerization of aniline and reduction of Ag from an ionic precursor. One advantage of this method is the strong particle-polymer interaction.¹⁷ This method is similar to that used by Kinyanjui et al.¹⁸ for PANI/Pt composites and should avoid the loss of conductivity associated with the reduction of metal ions into a preformed polymer. Multicomponent one-dimensional rod structures with tailorable electronic structures have recently been made by electrodeposition into

alumina templates by the Mirkin group.¹⁹ There have also been recent advances in fabricating nanorods containing metal cores surrounded by a polymer coat.^{20–22} Polyaniline and metal nanoparticle composites have been made by a one-pot synthesis^{23,24} but to the best of our knowledge this is the first time composite nanowires have been made in a single step inside an alumina template.

The morphologies of the nanowires were compared to those of Ag nanowires. Optical absorption, Raman, and FTIR were used to identify the chemical structure of the nanowires. The oxidation state of the polymer and the interaction between the Ag and PANI were also investigated.

2. Experimental Section

2.1. Materials. Aniline (99.5%), AgNO₃ (99%), H₂SO₄ (95–97%), and MgSO₄·7H₂O were purchased from Sigma-Aldrich Ltd. and the aniline monomer was purified by distillation in vacuum before use. The other chemicals were of reagent grade and used as received. Deionized water was used to make up the electrolyte solutions. ITO-covered glass was purchased from UQG (Optics) Ltd. Aluminum foil pieces (99%) purchased from Goodfellows Ltd. were used for the production of AAO.

2.2. Preparation of Silver and Composite Nanowires. Aluminum oxide membranes were used as nanotemplates in which the Ag and Ag/PANI composite nanowires were deposited. These templates were produced by the anodization of aluminum foil (99+%).^{25,26} Prior to anodization the sheets were degreased and the thermal oxide layer (~1–10 nm) was removed by dipping in hot chromic acid for 5–10 min. Surface inhomogeneities and scratches were removed by electropolishing in a mixture of hot phosphoric and sulfuric acids. Membranes with several different pore sizes were made with the following electrolytes: H₂SO₄ at 10–20 V for pores ~10–25 nm, H₂C₂O₄ at 40–80 V for pores ~40–100 nm, and H₃PO₄ at 100–140 V for pores ~100–170 nm. The pore diameter is linearly related to the anodizing voltage (1.2 nm/V). A voltage reduction was done to thin the barrier layer that inhibits anodic current during electrodeposition.²⁷

Electrochemical deposition was performed in a cell with the AAO template and a graphite rod as the working and counter electrodes in an AC setup.²⁶ Ag nanowires were deposited into AAO membranes (which were fabricated at 10, 20, 40, 80, and 140 V) at 9 V AC using an aqueous solution containing 1 g/L AgNO₃, 41 g/L MgSO₄·7H₂O and enough H₂SO₄ added until the pH of the solution was 2. Ag/PANI wires were also deposited into AAO membranes (made at 10, 20, 40, 80, and 140 V) at 9 V AC using the same electrolyte as above with the addition of 25.6 g/L aniline. The lengths of the nanowires can be varied from a few nanometers to tens of micrometers by changing the deposition time. Here deposition was carried out for 10 min in each case.

- (8) He, H.; Tao, N. J. *Electrochemical fabrication of metal nanowires*. In *Encyclopedia of nanoscience and nanotechnology*; Nalwa, H. S., Ed.; American Scientific Publishers: New York, 2003; Vol 10, pp 1–18.
- (9) Mallick, K.; Witcomb, M. J.; Scurrill, M. *Mater. Sci. Eng. B* **2005**, *123*, 181–186; *Eur. Polym. J.* **2006**, *42/3*, 670–675.
- (10) Pillalamarri, S. K.; Blum, F. D.; Tokuhira, A. T.; Bertino, M. F. *Chem. Mater.* **2005**, *17*, 5941–5944.
- (11) Doering, W. E.; Nie, S. J. *Phys. Chem. B* **2002**, *106*, 311–317.
- (12) Kreibitz, U.; Vollmer, M. *Optical properties of metal clusters*; Springer series in materials science; Springer Verlag: Berlin, 1995; Vol 25, pp 187–201.
- (13) Ghosh, K.; Maiti, S. N. *J. Appl. Polym. Sci.* **1996**, *60*, 323–327.
- (14) Wang, Y.; Yang, Q.; Shang, G. et al. *Mater. Lett.* **2005**, *59*, 3046–3049.
- (15) Yang, C.-H.; Chih, Y.-K.; Tsai, M.-S.; Chen, C.-H. *Electrochem. Solid State Lett.* **2006**, *9* (2), G49–G52.
- (16) Khanna, P. K.; Singh, N.; Charan, S.; Viswanath, A. K. *Mater. Chem. Phys.* **2005**, *92*, 214–219.
- (17) Kumar, R. V.; Mastai, X.; Diamant, Y.; Gedanken, A. *J. Mater. Chem.* **2001**, *11*, 1209–1213.
- (18) Kinyanjui, J. M.; Wijeratne, N. R.; Hanks, J.; Hatchett, D. W. *Chem. Mater.* **2004**, *16*, 3390–3398; *Electrochim. Acta* **2006**, *51*, 2825–2835.

- (19) Park, S.; J.-Lin, H.; Chung, S. W.; Mirkin, C. A. *Science* **2004**, *303*, 348–351; Park, S.; Chung, S. W.; Mirkin, C. A. *J. Am. Chem. Soc.* **2004**, *126*, 11772–11773.
- (20) Feng, X.; Liu, Y.; Lu, C.; Hou, W.; Zhu, J.-J. *Nanotechnology* **2006**, *17*, 3578–3583.
- (21) Chen, A.; Wang, H.; Li, X. *Chem. Commun.* **2005**, 1863–1864.
- (22) Huang, K.; Zhang, Y.; Long, Y.; Chen, J.; Han, D.; Wang, Z.; Niu, L.; Chen, Z. *Chem. Eur. J.* **2006**, *12*, 5314–5319.
- (23) Li, Z. F.; Swihart, M. T.; Ruckenstein, E. *Langmuir* **2004**, *20*, 1963.
- (24) Sarma, T. K.; Chattopadhyay, A. *J. Phys. Chem. A* **2004**, *108*, 7837–7842.
- (25) Masuda, H.; Fukuda, K. *Science* **1995**, *268*, 1466–1468.
- (26) Kröll, M. Ph.D. Thesis, Chem. Dept., University of Essen, Germany, 2000.
- (27) Furneaux, R. C.; Rigby, W. R.; Davidson, A. P. *Nature* **1989**, *337*, 147–149.

2.3. Preparation of PANI Nanowires and Films. Deposition of PANI into AAO membranes (10, 20, 40, 80, and 100 V as described above) by AC failed. An alternative method using DC was attempted. The nanowires were deposited into AAO templates prepared at 10 V in H_2SO_4 as described above. The aluminum foil and barrier layer at the back of the sample were removed by a solution of 0.2 M CuCl_2 in 3 M HCl (for Al) followed by 10% phosphoric acid (for the barrier layer). Gold was then sputtered onto the sample back to act as the working electrode. Platinum (Pt) was used as the counter electrode. Electrodeposition was carried out at constant potential (1.0 V DC) in a 25.6 g/L aniline solution to which concentrated H_2SO_4 was added until the pH of the solution was 2. Film deposition was achieved in a two-electrode cell with graphite electrodes. The ITO was attached to the working electrode. The electrolyte solution was the same as that used to make the PANI wires. Electropolymerization was carried out at constant potential by potentiostatic deposition at 1.0 V for 10 min.

2.4. Characterization. The phase and crystallographic structure of the composite nanowire arrays were determined by X-ray diffraction (XRD) using a Philips PW3040/60 X'Pert PRO in θ - 2θ coupled mode. XRD was done on an Ag nanowire array for comparison.

The surface morphologies of the samples were observed by scanning electron microscopy (SEM) at an accelerating voltage of 15 kV on an S-450 Hitachi High Technologies. Small pieces of the samples were attached with conducting glue to aluminum sample holders and covered with 10 nm of sputtered gold. The surface of the samples was previously etched with 0.2 M NaOH to expose the nanowires. The sizes of Ag/PANI wires were determined with an HITACHI H-7000 (TEM) operated at 100 kV and a FEI TECNAI F20 (HRTEM) operated at 200 kV. TEM samples were prepared by placing a few drops of a suspension of the wires in filtered deionized water onto a holey carbon grid and drying them overnight in a vacuum oven at 40 °C. The nanowires were extracted by shaking in a solution of 0.1 M NaOH and 30 g/L PVP for 12–24 h, followed by washing several times in Millipore filtered deionized water. UV-vis spectra were recorded in the wavelength range 300–1000 nm on a Perkin-Elmer Lambda 900 UV-vis/NIR. The aluminum foil was first removed from the back of the membrane by a solution of 0.2 M CuCl_2 in 3 M HCl.

Raman and FTIR spectroscopy confirm the presence of polyaniline. These were carried out on a Jobin Horiba LabRAM HR and a Perkin-Elmer Spectrum 1 FTIR with a universal ATR sampling accessory, respectively. Omnic software was used for analysis.

3. Results and Discussion

3.1. Morphology. The SEM image (Figure 3b) shows that the nanowires are fibers, which closely resemble PANI nanowires (Figure 3a). Their lengths varied between 1 and 2 μm and the pore filling was approximately 80%.

TEM images (Figure 4a) show that they are polycrystalline as the different domains of the nanowire crystals give rise to different contrasts in the TEM. They are surrounded by a layer of amorphous material (lighter shading). It is also apparent that the nanowires remain parallel to each other even when they are removed from the AAO matrix. Figure 4b shows a TEM image of pure Ag nanowires. They have a similar structure to the interior of the composite wires with no external shading. Thus, the exterior shading in the composite wires is probably due to a coating of PANI and suggests that as the Ag nanowires are formed along the pores

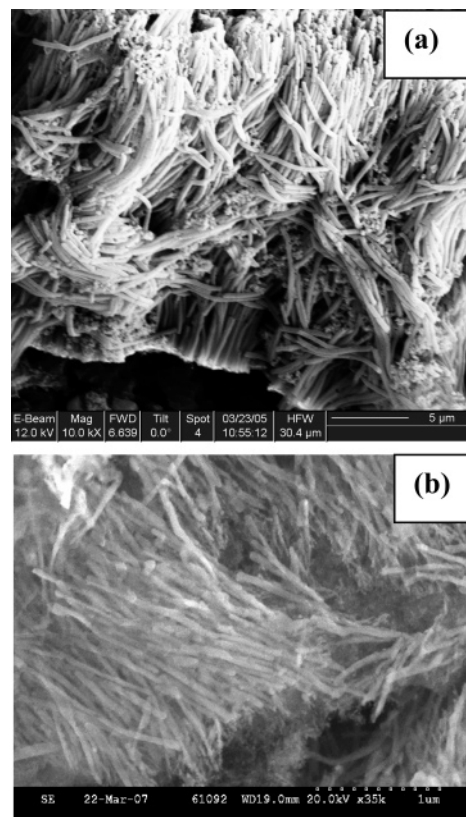


Figure 3. SEM of (a) PANI nanowires and (b) composite nanowires in AAO membranes (etched with NaOH).

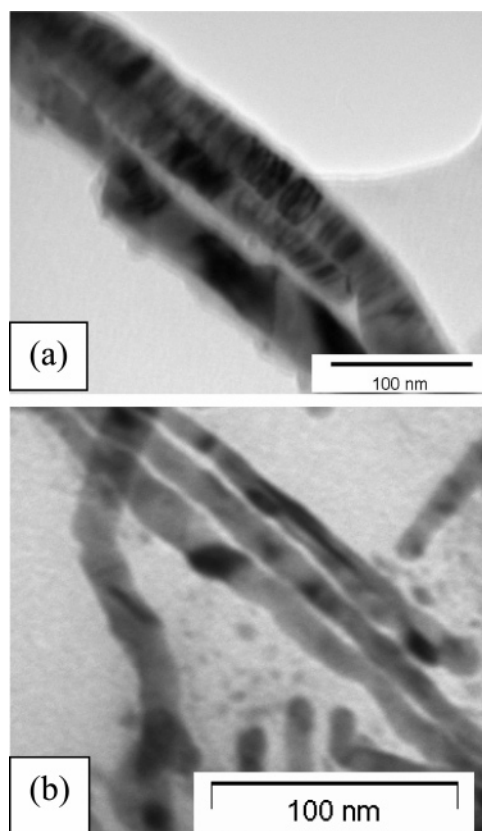


Figure 4. TEM of (a) composite (b) silver nanowires extracted from AAO templates.

of the AAO template they take a coating of polymer with them.

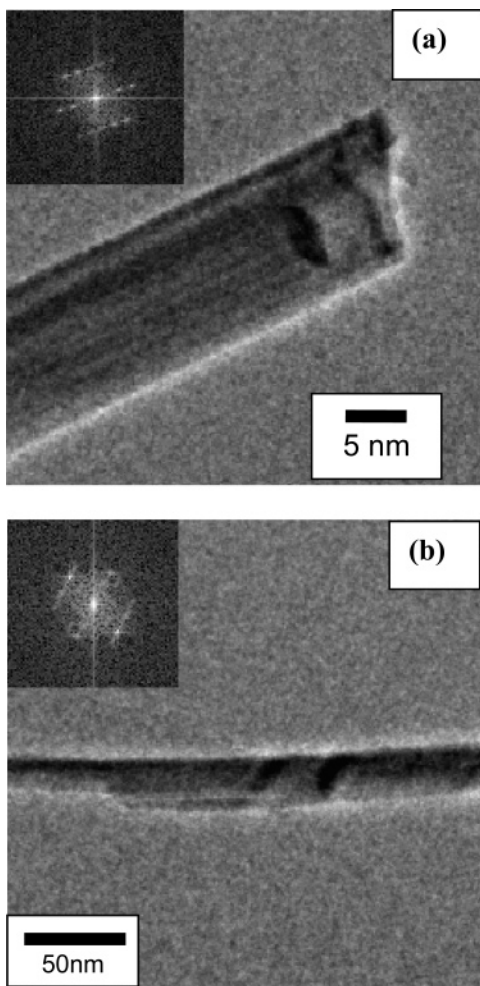


Figure 5. HRTEM of composite nanowires extracted from AAO templates made at 15 V (a) and 40 V (b) with corresponding diffraction patterns (insets).

HRTEM supports these findings (Figures 5a and 5b). Here the shading is seen as a white halo of amorphous carbon around the Ag core; this halo was always present on going through a set of 20 images in a focal series (1 nm step), thus showing that it is not an artifact due to focal inconsistencies. The corresponding diffraction patterns, as obtained by fast Fourier transforming (FFT) the shown images, are in the insets. The inset on Figure 5a is a selected area diffraction pattern (FFT) made on a 15 nm diameter nanowire. This shows the highly crystalline nature of the core where all the Ag crystal planes are allocated as follows: top row left to right 210, 110, 010, 110, 210; middle row left to right -300 , 200, 100, 100, 200, -300 ; bottom row left to right 2 -10 , 1 -10 , 0 -10 , 1 -10 , 2 -10 . Figure 5b is of a 40 nm diameter nanowire which is taken at a lower magnification so the halo is included in the diffraction pattern (inset). As well as the diffraction spots due to silver, it also shows a bright ring which is indicative of amorphous carbon due to the PANI coating.

A more detailed study of the morphology of different sized nanowires is being undertaken to see if the confinement effect of different size pores affects the molecular organization of the nanowires as in the case of Wu et al.²⁸ Preliminary investigation shows that the size of the polymer coating

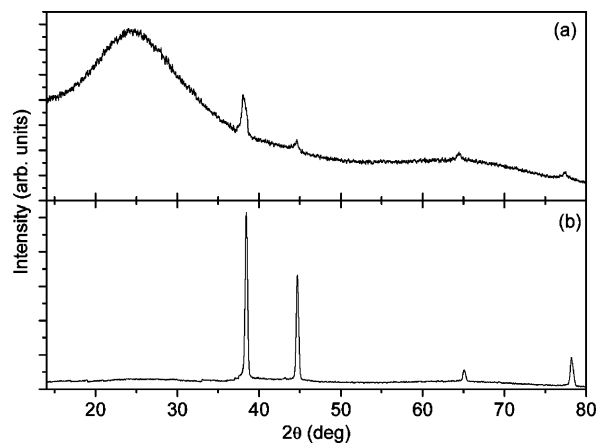


Figure 6. XRD of the composite array (a) compared to Ag nanowire array (b).

varies with the size of the nanowires, but not in a systematic manner.

3.2. Structural Characterization. **3.2.1. X-ray Diffraction (XRD).** The crystalline nature of the composite wires was determined from XRD analysis. An X-ray diffraction pattern of a composite nanowire array is shown in Figure 6a. A broad peak centered at $2\theta = 25^\circ$ is observed and can be ascribed to weak ordering parallel to the polymer chain. Sharp peaks centered at $2\theta = 38^\circ$, 45° , 66° , and 77° are also observed corresponding to (111), (200), (220), and (311) silver planes. All the peaks can be indexed to face-centered cubic silver belonging to space group $Fm\bar{3}m$ [225]. The silver is preferentially oriented along the (111) plane. Crystallite sizes can be calculated from Scherrer's equation:

$$D = k\lambda/\beta \cos \theta$$

where λ is the X-ray wavelength (0.1540 nm), K is the shape factor ≈ 0.89 , D is the average diameter of the crystals (in Armstrong units), θ is the Bragg angle (in degrees), and β is the broadening measured at half-height and expressed in units of 2θ .¹⁵

Using our values at $2\theta = 77^\circ$ gives $D = 10$ nm which agrees well with TEM results.

Figure 6b shows the X-ray diffraction pattern of pure silver nanowires in AAO where the same peaks corresponding to (111), (200), (220), and (311) silver planes are clearly seen.

3.2.2. Raman Spectroscopy. Raman spectroscopy was used to confirm the presence of PANI. Raman microprobe spectroscopy has the advantage that a spectrum of the nanowires can be taken without removing them from the alumina matrix. The composites show all the characteristic peaks for PANI (Figure 7 and Table 1); however, there are some subtle differences between these spectra and those of pure PANI, which give us an insight into the oxidation state of PANI in the composite.

For example, the bands between 415 and 806 cm^{-1} show slight shifts and broadening in the composite. This is indicative of the weakening of interchain interactions.²⁹

(28) Wu, Y.; Cheng, G.; Katsov, K.; Sides, S. W.; Wang, J.; Ting, J.; Fredrickson, G. H.; Moskovits, M.; Stucky, G. D. *Nat. Mater.* **2004**, *3*, 816–822.

(29) Abdiryim, T.; Xiao-Gang, Z.; Jamal, R. *Mater. Chem. Phys.* **2005**, *90*, 367–372.

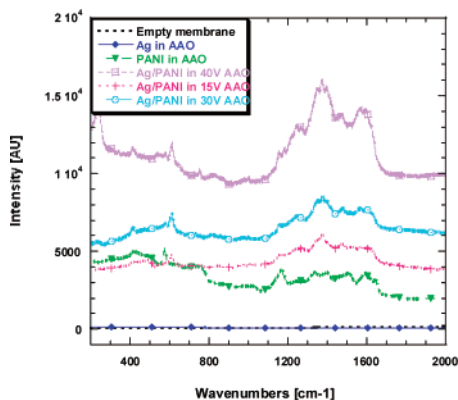


Figure 7. Raman spectra of composite nanowire arrays in AAO compared to an array of PANI in AAO, a silver nanowire array in AAO, and an empty AAO template (excitation $\lambda = 633$ nm).

Table 1. Assignments for Raman Bands in a Composite Sample in AAO Membrane

region [cm ⁻¹]	vibration
415	C–N–C torsion and out of plane deformation of benzenoid ring
480, 580	CH out-of-plane and aniline deformation mode
523, 615, 806	deformation of benzenoid or quinoid rings
1165	CH bending of benzenoid rings
1340	C–N: stretching of modes of quinoid rings
1475	–C=N stretching modes of quinoid ring
1410, 1595	–CC stretching of benzenoid rings

Spectral changes between 1100 and 1700 cm⁻¹ are characteristic of changes in oxidation state. The band due to the C–H bending of benzenoid-like aromatic rings in PANI is decreased to 1165 cm⁻¹ in the composites due to progressive oxidation of the polymer and the formation of quinoid-like rings;³⁰ this band is also present in the PANI array at 1170 cm⁻¹ and has a strong intensity. This may be due to the presence of the sulfate group.³¹ Bands in the region 1250–1300 cm⁻¹ are stronger in the composite and can be assigned to C–N stretching of the secondary aromatic amine, indicative of the emeraldine salt phase of PANI.³³ Bands in the 1300–1400 cm⁻¹ region are due to stretching vibrations of C–N+ fragments having an intermediate single-to-double bond order and coupled to an aromatic ring.³² The appearance of one or two bands in this range depends on whether the polymer is in the fully reduced or oxidized form or in the half-oxidized emeraldine form. Our results show that the PANI array has two bands at 1335 and 1405 cm⁻¹ typical of the emeraldine salt form; these two bands are also present in the composites (at 1350 and 1380 cm⁻¹), indicating that although it is also in the emeraldine salt state it is not identical to PANI. Ring sulfonation also affects the polaronic C–N+ vibration bands in this region.^{31,33} There are also some slight differences in the higher frequency regions. These bands are due to the stretching modes of the benzenoid and quinoid rings. The band located at 1475 cm⁻¹ in the composite wires corresponds to the stretch vibrations of the

(30) Quillard, S.; Berrada, K.; Louarn, G.; Lefrant, S.; Lapkowski, M.; Pron, A. *N. J. Chem.* **1995**, *19*, 365–374.

(31) Niaura, G.; Mazeikiene, R.; Malinaukas, A. *Synth. Met.* **2004**, *145*, 105–112.

(32) Boyer, M. I.; Quillard, S.; Louarn, G.; Froyer, G.; Lefrant, S. *J. Phys. Chem. B* **2000**, *104*, 8952–8961.

(33) Yue, J.; Epstein, A. J.; MacDiarmid, A. G.; Skotheim, T. A. *Mol. Cryst. Liq. Cryst.* **1990**, *189*, 255–261.

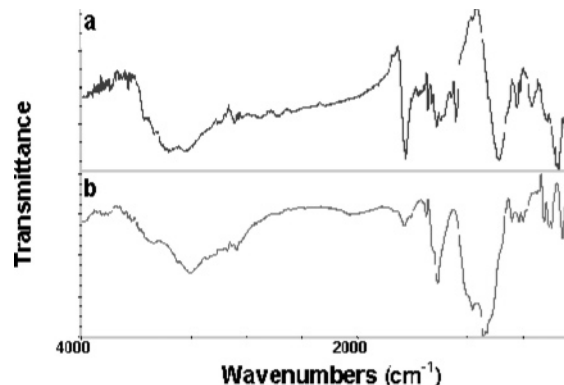


Figure 8. FTIR of composite wires extracted from an AAO membrane (a above) and PANI film (b below).

Table 2. Assignments for FTIR Bands in a Composite Sample Extracted from a 40 V AAO Membrane

region [cm ⁻¹]	assignment
3471	non-hydrogen-bonded N–H stretching vibration
3237	hydrogen-bonded N–H stretching vibration
1753	C=N vibrational modes
1545	C=N and C=C stretching deformation from quinoid rings
1488	C=C stretching deformation from benzenoid rings
1285	C–N stretching of secondary aromatic amine

C=N double bond, highly coupled to the quinoid ring.³⁴ This appears as a shoulder in the PANI sample and the band at 1595 cm⁻¹ due to C–C stretching of the benzenoid-like rings is stronger in the PANI sample, indicating that it is less oxidized than the composite. Finally, the Raman scattering signal is enhanced in the composite samples due to surface-enhanced Raman scattering (SERS) of the Ag particles, which also confirms the presence of Ag in the composites. The enhancement varies with the size of the nanowires as shown in Figure 7. A systematic study is being undertaken to quantify this.

3.2.3. Fourier Transform Infrared Spectroscopy (FTIR). Infrared spectroscopy can be used to study the oxidation state of PANI. Composite nanowires were extracted from the alumina template for FTIR analysis. As this involves treatment with sodium hydroxide (NaOH), the sulfuric acid (H₂SO₄) doped PANI will be changed to its undoped form. This is reflected in the IR spectrum. A comparison of the spectra of these composite wires and that of a film of PANI made with H₂SO₄ in the electrolyte can give us some insight into the doping effect of the H₂SO₄ and the interaction of Ag with PANI.

The nanowire composites show all the characteristic peaks for PANI (Figure 8a and Table 2). The FTIR of a PANI film is taken for comparison (Figure 8b).

The intensity of the free N–H bond (3357 cm⁻¹) increases while that of the hydrogen-bonded N–H stretching (3237 cm⁻¹) decreases in the composite, indicating a weakening of the hydrogen bonding between amine and imine groups. This could be due to the protonation of PANI due to the acid dopant followed by formation of co-ordination bonds between the silver metal ions and polymer nitrogen atoms.

The spectrum shows many vibrational modes due to C–N (e.g., 1653, 1545, 1488, and 1285 cm⁻¹); this is because the

(34) Ibrahim, M.; Koglin, E. *Acta Chim. Slov.* **2005**, *52*, 159–163.

polymer contains both amine and imine units so each ring will give rise to a different vibrational mode.³⁴ The absence of the band at 1189 cm^{-1} in the composite wires, which is due to protonated chain vibrations, is notable.³⁵ This band is characteristic of protonated chain vibrations $Q = \text{NH}^+ - \text{B}$ or $\text{B} - \text{NH}^+ - \text{B}$ ($Q = \text{quinoid}$, $\text{B} = \text{benzenoid}$ units of polymer) which can hydrogen bond to the $-\text{NH}-$ or $=\text{N}-$ groups in PANI. This bonding is weakened when the Ag is incorporated into the polymer matrix (as Ag^+ is reduced to Ag^0 and the $-\text{NH}-$ groups of the polymer chain are oxidized to $-\text{N}=\text{}$). FTIR analysis of PANI fibrils made by Wang et al.⁶ also show a stretching vibration mode at 1124 cm^{-1} similar to our films of PANI. Further evidence of the two different C–N bond link ways in the composites is the presence of a C–N stretch at 1285 cm^{-1} .⁷ Previous studies by Hasik et al.³⁶ show that similar interaction of PANI with Pd compounds leads to the reduction of Pd^+ to Pd^0 with simultaneous oxidation of the polymer chain.

Doping transforms a certain amount of the aminobenzene group into quinoid moiety in the polymer. Characteristic bands associated with benzenoid (1488 cm^{-1}) and quinoid (1545 cm^{-1}) phenyl rings can be used to estimate the oxidation state of the polymer by integrating these IR bands.³⁷ However, in the composite wires the quinoid bands are very small and masked by the large C=N vibrational modes at 1653 cm^{-1} . It has been reported that in doped PANI many of the key bands corresponding to the aromatic rings are shifted to lower frequencies.³⁸ In fact, many of the bands in the PANI sample are red-shifted compared to the composite wires because of the acid dopant (e.g., $3237\text{ cm}^{-1} > 3187\text{ cm}^{-1}$, $2873\text{ cm}^{-1} > 2857\text{ cm}^{-1}$, $1653\text{ cm}^{-1} > 1641\text{ cm}^{-1}$, $1488\text{ cm}^{-1} > 1487\text{ cm}^{-1}$, $1418\text{ cm}^{-1} > 1414\text{ cm}^{-1}$). There are also some extra bands due to the absorption of $-\text{SO}_3\text{H}$ groups.^{39–40}

There is also a difference in the position of the CH out-of-plane bands. These occur at 837 , 724 , 609 , and 536 cm^{-1} in the composite and 862 , 790 , 728 , 647 , 572 , and 543 cm^{-1} in PANI.

3.2.4. UV–Vis Absorption Spectroscopy. The characteristic absorption bands for the pristine undoped EB form of PANI are 336 and 600 nm .⁴⁰ PANI salts show three transitions 306 – 324 nm ($\pi-\pi^*$ transition of benzenoid rings), 402 – 412 nm (polaron- π^* transition), 828 – 835 nm (π -polaron transition).^{40,41} The ratio of the absorbencies at approximately 800 and 400 nm indicates the doping level of polyaniline.²⁹ However, for doped PANI nanowires the 330 nm peak is absent and bands at 430 and 900 nm with a long tail are observed.^{10,40} Our results for a film of PANI on ITO (Figure 9) show a shoulder at 450 nm and a broad peak at around

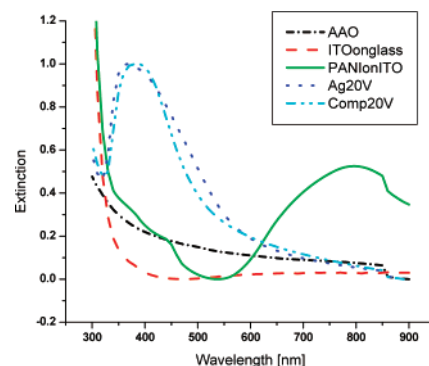


Figure 9. UV vis spectra of composite nanowires electrodeposited at 20 V ac in AAO compared to Ag nanowires in AAO (made under the same conditions, i.e., 20 V ac), a film of PANI on ITO, ITO on glass, and an empty AAO.

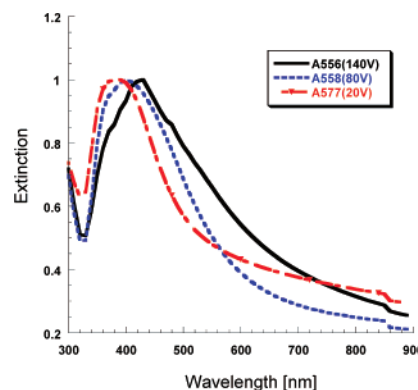


Figure 10. UV–vis spectra of composite arrays in AAO membranes (made at 20 , 80 , and 140 V).

800 nm , which is typical of the half-oxidized emeraldine base.

Silver nanowires show a maximum absorption peak at 382 nm corresponding to a surface plasmon resonance due to the transverse oscillation of electrons along the nanowires.⁴² This overlaps with the absorption band of polyaniline so it is difficult to differentiate them.¹⁰ Khanna et al. observed that the bands at 400 – 420 nm due to the benzenoid rings of the PANI are overlapped and red-shifted due to the presence of nanosilver.¹⁶ Our results for the composite nanowires are similar (see Figure 9). This figure shows that the absorption of the composite wires in AAO matches that of the Ag wires but the position of the absorption maximum is red-shifted, indicating that the wires have a different electronic environment than the noncoated wires. The absorption bands at 630 and 835 nm corresponding to the EB and ES forms of PANI are absent in the composite, indicating that the absorption is totally dominated by silver.

The λ_{max} of the composite wires also depends on their diameter.

Figure 10 illustrates that λ_{max} is shifted to higher wavelengths and the width of the absorption peak increases with increasing wire diameters. This is similar to studies done on Ag nanowires⁴³ and is probably due to the broad plasmon

(35) Hasik, M.; Drelinkiewicz, A.; Wenda, E.; Paluszkiwicz, C.; Quillard, S. *J. Mol. Struct.* **2001**, *596*, 89–99.

(36) Hasik, M.; Drelinkiewicz, A.; Choczyski, M.; Quillard, S.; Pron, A. *Synth. Met.* **1997**, *84*, 93–94.

(37) Tang, J.; Jing, X.; Wang, B.; Wang, F. *Synth. Met.* **1988**, *24*, 231.

(38) Mathai, C. J.; Saravanan, S.; Anatharaman, M. R.; Venkitachalam, S.; Jayalekshmi, S. *J. Phys. D.: Appl. Phys.* **2002**, *35*, 2206–2210.

(39) Gemeay, A. H.; Mansour, I. A.; El-Sharkawy, R. G.; Zaki, A. B. *Eur. Polym. J.* **2005**, *41*, 2575–2583.

(40) Zhang, L.; Wan, M. *Nanotechnology* **2002**, *13*, 750–755.

(41) Lu, X.; Gao, H.; Chen, J.; Chao, D.; Zhang, W.; Wei, Y. *Nanotechnology* **2005**, *16*, 113–117.

(42) Caswell, K. K.; Bender, C. M.; Murphy, C. J. *Nano. Lett.* **2003**, *3/5*, 667–669.

(43) Kröll, M.; O'Flaherty, S. M.; Blau, W. J. Presented at SPIE conference Opto-Ireland, Galway, 2002.

resonance that is red-shifted with increasing wire diameter due to the increasing importance of multipole excitations.

3.3. Mechanism Formation. The formation mechanism of these Ag/PANI nanocables is probably similar to that of Huang et al.²² for the synthesis of AuPpy nanowires and Kinyanjui et al.¹⁸ for the electrochemical synthesis of Pt/PANI composites. We propose that sulfuric acid acts as a dopant and Ag as a catalyst in the polymerization process. The aniline is first protonated by H₂SO₄ to form a protonated anilinium cation. The Ag anion then acts as an electron acceptor and is reduced to Ag⁰ while oxidative polymerization of aniline occurs. In acidic media the PNB form of PANI is reduced back to ES, thus enabling further reduction of Ag⁺ to Ag⁰.⁴⁴ The Ag particles act as nucleation sites for the oxidative formation of PANI which surrounds the metal core. Diffusion of the composite into the membrane then occurs as the neutrality of the system is restored. Thus, the growth process of the silver nanowires and the polymerization of the polymer sheath continue simultaneously. This is similar to the process which occurs during the photochemical synthesis of polyaniline.^{16,45}

Conclusions

The synthesis of Ag/PANI nanowires was achieved by simultaneous electrodeposition of Ag and PANI into the nanopores of an alumina template. This is done by oxidative polymerization of aniline and reduction of silver nitrate to silver nanowires. Deposition of PANI into these templates by the same method was unsuccessful which implies that Ag is acting as a catalyst for the polymerization of aniline in such cases.

SEM shows the fibrous nature of the composite nanowires and TEM shows they resemble Ag nanowires. HRTEM indicates that they consist of a metal core surrounded by polymer coating, i.e., a nanocable. Such structures are usually made by template processing or layer deposition (ref 46 and

references therein). XRD, Raman, and FTIR spectroscopy were used to characterize the structure and chemical composition of the wires. Raman evidence indicated a change in the oxidation state of the PANI in the composite (formation of quinoid rings and increased C–N stretching). The evidence from FTIR indicates that there is some interaction between and the nitrogen head groups of the polyaniline (differences in the N–H bands due to hydrogen bonding, weakening of the protonated chain vibrations, and a shift in the semi-quinoid C–N stretch in the composite). UV–vis spectroscopy also supports the proposed formation mechanism of the nanocables. If the Ag was dispersed as clusters within the PANI, the surface plasmon resonance of Ag would be missing.⁴⁷ The peak at 400 nm indicates that elemental silver is formed at the same time as PANI. As the aniline polymerizes, it is trapped by the growing crystal Ag nanowires, which then grow orientationally along the pores of the AAO template because of the trapping effect of the template.⁴⁸ Many studies give evidence of the directional aggregation of clusters of particles leading to the directional growth of nanowires.^{28,49–50} To our knowledge this is the first composite nanowire fabricated in a one-pot method inside an alumina template. This has many advantages as the nanocables can be used as an array inside the template or extracted and used in other systems. Other metal/polymer composite nanocables could be prepared in a similar way. Work on Cu/PANI composites is already in progress.

Acknowledgment. This work was funded by Science Foundation Ireland and the Higher Education Authority, Ireland. The authors thank David John and Neal Leady from the Centre for Microscopy and Analysis, TCD for some TEM and SEM measurements, Peggy Brehon from the School of Chemistry, TCD for help with FTIR measurements, and Ramesh Babu from Materials Ireland, School of Physics, TCD, for useful discussions.

CM071102S

(44) O'Mullane, A. P.; Dale, S. E.; Macpherson, J. V.; Unwin, P. R. *Chem. Commun.* **2004**, 1606–1607.

(45) de Barros, R. A.; de Azevedo, W. M.; de Aguiar, F. M. *Mater. Char.* **2003**, *50*, 131–134.

(46) Chen, A.; Wang, H.; Li, X. *Chem. Commun.* **2005**, 1863–1864.

(47) Sun, Y.; Yin, Y.; Mayers, B. T.; Herricks, J.; Xia, Y. *Chem. Mater.* **2002**, *14*, 4736–4745.

(48) Sun, X.-Y.; Xu, F.-Q.; Li, Z.-M.; Zhang, W.-H. *Mater. Chem. Phys.* **2005**, *90*, 69–72.

(49) Cui, S.; Liu, Y.; Yang, Z.; Wei, X. *Mater. Des.* **2005**, *28*, 722–725.

(50) Gu, X.; Nie, C.; Lai, Y.; Lin, C. *Mater. Chem. Phys.* **2006**, *96*, 217–22.